# System-size resonance in a binary attractor neural network

M. A. de la Casa,[1,*] E. Korutcheva,[1,†] J. M. R. Parrondo,[2] and F. J. de la Rubia[1]
[1]*Departamento Física Fundamental, Universidad Nacional de Educación a Distancia, c/Senda del Rey 9, 28080 Madrid, Spain*
[2]*Grupo Interdisciplinar de Sistemas Complejos (GISC) and Departamento Física Atómica, Molecular y Nuclear, Universidad Complutense, 28040 Madrid, Spain*
(Received 31 May 2005; published 30 September 2005)

System size resonance (SSR) is a phenomenon in which the response of a system is optimal for a certain finite size, but poorer as the size goes to zero or infinity. In order to show SSR effects in binary attractor neural networks, we study the response of a network, in the ferromagnetic phase, to an external, time-dependent stimulus. Under the presence of such a stimulus, the network shows SSR, as is demonstrated by the measure of the signal amplification both analytically and by simulation.

DOI: 10.1103/PhysRevE.72.031113 PACS number(s): 05.40.Ca, 05.70.Ln, 07.05.Mh

## I. INTRODUCTION

In the last years, a huge amount of literature has been accumulated on the counterintuitive effect of the noise as a source of order. This ordering effect has been reviewed in the context of both zero-dimensional systems [1] and spatially extended systems [2]. Of special interest for the present paper is the phenomenon of stochastic resonance in which the response of a nonlinear system to the action of a weak signal is enhanced, and not hindered as it could be naively expected, by the addition of an optimal amount of noise [3,4]. Closely related to stochastic resonance is another phenomenon that recently appeared in the literature, the so-called system size resonance (SSR) [5]. In SSR, the presence of noise in a system of finite size close to a second-order phase transition gives rise to the appearance of an optimal size for the system to adapt to an external field [5–7]. SSR has attracted some attention in the last couple of years [8–11]. A general nonequilibrium potential framework was recently proposed by the study of SSR [12]. It was shown that the analysis of the potential can give a clear physical interpretation of the phenomenon. It has been shown that the SSR even arises in opinion formation models [13].

Inspired by the applications of stochastic resonance to cognitive processes [14–18], as well as the modulelike organization of the neurons in the human brain, we are searching for a tradeoff at mesoscale level between the size of these formations and the performance of the system, which forms the basis of the principles of self-organization. We show that SSR can operate in a model of associative memory as is the Hopfield binary neural network [19], improving its ability to follow a time-dependent stimulus. We focus on the simplest case of a Hopfield network storing two patterns presented periodically to the system and show that there is always an optimal size of the neural network, for which the amplification of the signal is maximal. The model we chose gives a clear physical interpretation of the SSR phenomenon and serves as a basis for the study of the processes in more complex real systems at mesoscopic level.

The paper is organized as follows. In Sec. II we introduce the model. The corresponding thermodynamic analysis is given in Sec. III and the analytical derivation of the phenomenon of system size resonance is presented in Sec. IV. In Sec. V we analyze the results obtained both analytically and by simulation. Finally, in Sec. VI we give our conclusions.

## II. THE MODEL

In this paper, we study the presence of SSR effects in Hopfield's model of a binary attractor neural network [19], given by the following Hamiltonian:

$$\mathcal{H} = -\frac{1}{N}\sum_{i<j} J_{ij} s_i s_j - h\sum_i \xi_i^{\mu(t)} s_i, \tag{1}$$

where $N$ is the number of (binary) neurons, $s_i$, $i=1,\ldots,N$ and $\xi_i^{\mu}$, $i=1,\ldots,N$, $\mu(t)=1,2$ are two (binary) patterns the system is trained with.

The neurons are coupled to each other according to the Hebb's rule [20] by

$$J_{ij} = \sum_{\mu=1}^{2} \xi_i^{\mu}\xi_j^{\mu}. \tag{2}$$

The first term on the right-hand side of Eq. (1) gives the coupling between pairs of neurons. The second term gives the coupling with an external field of intensity $h$, which is periodic in time. The action of this field is to periodically drive the system to the state $s_i=\xi_i^1$ for a time interval $T$ and then to $s_i=\xi_i^2$ during another interval $T$. This field plays the role of an external dynamic stimulus driving the network to remember periodically the two patterns.

Another relevant parameter is the Hamming distance between the patterns, defined as

$$d = \frac{1}{2N}\sum_{i=1}^{N} |\xi_i^1 - \xi_i^2|. \tag{3}$$

The distance $d$ is the fraction of sites in which both patterns are different. It varies between 0, when both patterns are

*Email address: macasa@fisfun.uned.es
†Also at G. Nadjakov Institute of Solid State Physics, Bulgarian Academy of Sciences, 1784 Sofia, Bulgaria.

 

equal at every site, and 1 when they are different.

This system has been extensively studied in the literature [21], mainly in the thermodynamic limit ($N\to\infty$). The role of a finite size has almost only been studied in order to find finite size corrections to infinite-size results [22]. Meanwhile we will keep $N$ explicitly finite and will focus on the effect of the finite size on the response of the system to an external time-dependent stimulus.

### III. THERMODYNAMICAL ANALYSIS

In the thermodynamic limit, $N\to\infty$, the model described by Eq. (1), undergoes a second-order phase transition at a critical temperature $\beta_c=1$ [23]. The results presented in [5] on the Ising model and the $\phi^4$ model suggest that this phase transition could be a good test ground to study the appearance of SSR effects in a broader and richer context.

The first step in our study of the system is to obtain an exact expression for the free energy of the system in terms of the distance $d$ and the order parameter, which is the usual overlap between patterns and neurons,

$$m_\mu = \frac{1}{N}\sum_i \xi_i^\mu s_i. \tag{4}$$

The expression for the free energy of the system, including the action of the stimulus, reads

$$\mathcal{F} = -\frac{N}{2}(m_1^2+m_2^2) - hm_{\mu(t)} - \frac{1}{\beta}\log\left[\binom{N(1-d)}{\frac{N}{4}(m_1+m_2+2(1-d))} \times \binom{Nd}{\frac{N}{4}(m_1-m_2+2d)}\right], \tag{5}$$

where the second term is the entropic contribution. However, the two order parameters $m_1$ and $m_2$ are not independent. A more convenient pair of magnitudes can be defined as follows: $r$ is the fraction of bits where $\{s_i\}$ coincides both with pattern 1 and 2; $p$ is the fraction of bits where $\{s_i\}$ coincides with pattern 1 and differs from pattern 2. In Fig. 1 we have plotted a schematic representation of the two patterns and the quantities $p$ and $r$. Taking into account that $m_\mu$ is the fraction of common bits minus the fraction of different bits between the network and pattern $\xi^\mu$, from Fig. 1 one immediately obtains

$$m_1 = 2r+2p-1; \quad m_2 = 2r+2d-2p-1. \tag{6}$$

Also from this figure, it is easy to see that $r$ and $p$ are independent and can take on any value in the rectangle: $r\in[0,1-d]$, $p\in[0,d]$. Moreover, in terms of $r$ and $p$, the free energy of the system for $h=0$ can be written as

$$\mathcal{F} = \mathcal{F}_r + \mathcal{F}_p \tag{7}$$

with

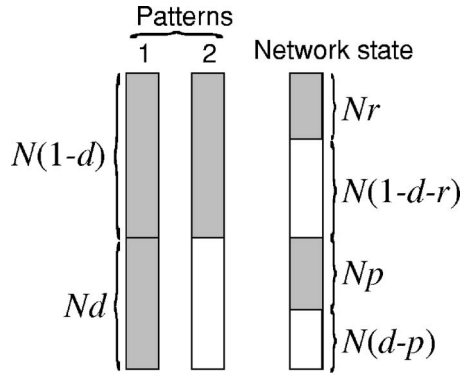


FIG. 1. Schematic representation of the two patterns and the state of the network. The upper part of the patterns represents the $N(1-d)$ coincident bits between the patterns. $Nr$ is the number of bits that the network has in common with both patterns, whereas $Np$ is number of bits in the network coinciding with pattern 1 and different from pattern 2.

$$\mathcal{F}_r = -4N\left(r-\frac{1-d}{2}\right)^2 - \frac{1}{\beta}\log\binom{N(1-d)}{Nr}$$

$$\mathcal{F}_p = -4N\left(p-\frac{d}{2}\right)^2 - \frac{1}{\beta}\log\binom{Nd}{Np}. \tag{8}$$

At zero temperature, the free energy has four equilibria, located at the corners of the available rectangle in the parameter space, i.e., $r=0$, $1-d$, and $p=0,d$. Two of the four equilibrium states, $r=1-d$, $p=0,d$, exactly reproduce the two patterns. The other two minima, $r=0$, $p=0,d$, are the negatives of the stored patterns. Figure 2(a) shows a typical landscape of the free energy in the $(r,p)$ plane for low temperatures ($\beta=2$, $d=0.7$).

If we increase the temperature, the four minima shift to the middle point of the rectangle $r=(1-d)/2$ and $p=d/2$. In the thermodynamic limit, the system undergoes two second-order phase transitions at $\beta_{c,r}=1/(2-2d)$ and $\beta_{c,p}=1/(2d)$. In each transition the minima collide into either $r=(1-d)/2$ or $p=d/2$, which corresponds, respectively, to a completely disordered state in the region of common and distinct bits between the two patterns (see Fig. 1). The ability of the network to distinguish between the two patterns sensibly depends on which of the two transitions occurs first. The phase diagram of the system can be seen in Fig. 3.

For $d=0$, $\beta_{c,p}=\infty$, as the two patterns coincide and there are no different fractions of bits between them for any finite temperature. The same is true for $d=1$ when $\beta_{cr}=\infty$, as there are no common fractions between $\{s_i\}$ and both patterns.

If $d<0.5$, i.e., if the two patterns share more than one-half of the bits, $\beta_{c,p}>\beta_{c,r}$. Consequently, when the temperature increases from absolute zero the first transition occurs for the variable $p$, i.e., in the region of distinct bits. This means that for temperatures $\beta\in[\beta_{c,r},\beta_{c,p}]$, the system only exhibits two minima with $p=d/2$, i.e., with $m_1=m_2$ [see Eq. (6)]. One of these two minima approximately reproduces the common bits of the two patterns, whereas the distinct bits are completely disordered. The other minimum is just the nega-

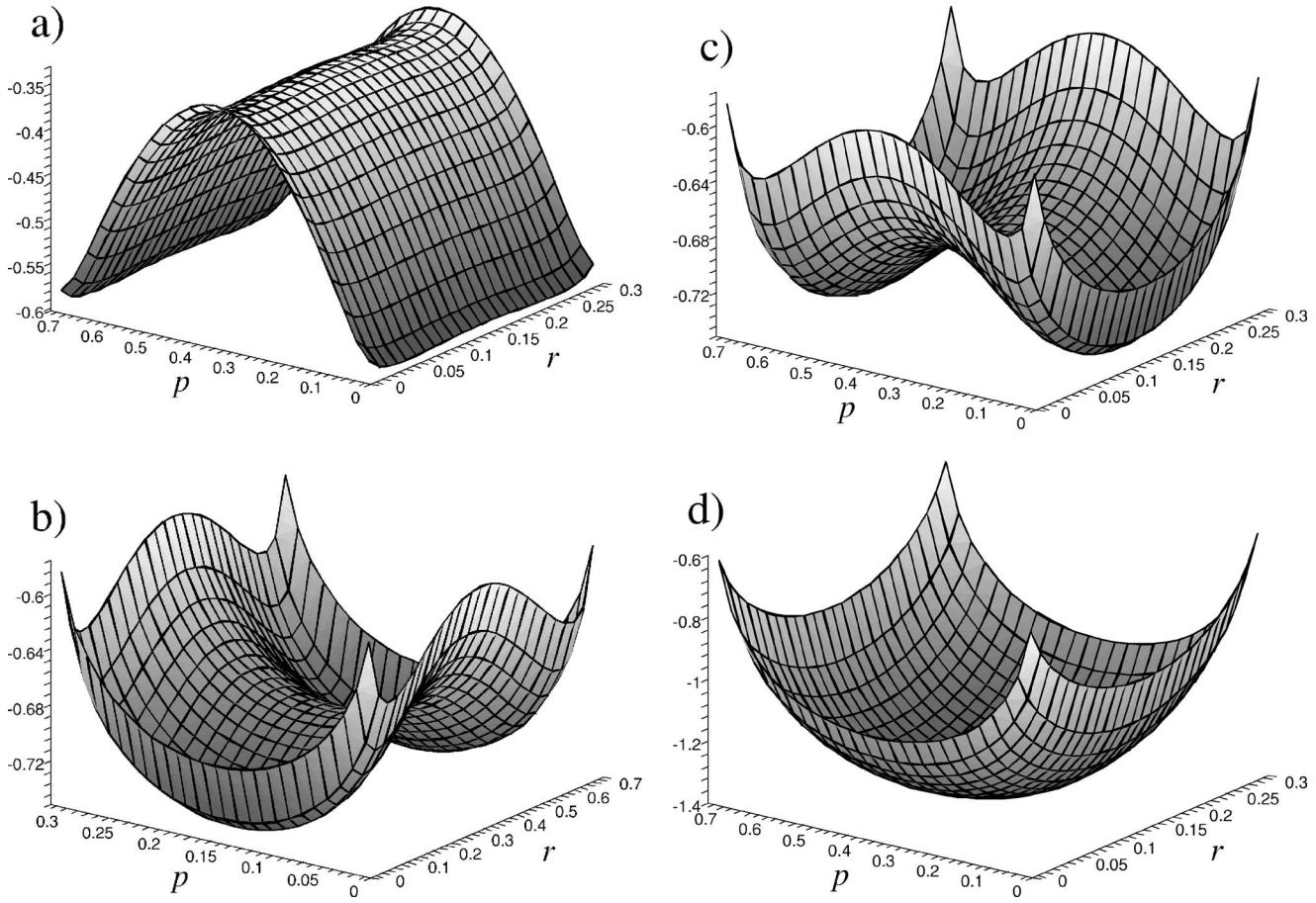


FIG. 2. The free energy landscape for $h=0$ and $N=10\,000$. (a) *Low temperature*, $\beta=2$, $d=0.7$: The free energy presents four minima, corresponding to the two stored patterns and their respective negatives. (b) *Medium temperature, similar patterns*, $\beta=1$, $d=0.3$: There are two equilibrium states with $p=d/2$, i.e., with $m_1=m_2$. One of the minima reproduces the common bits of the two patterns whereas the other one is its negative. (c) *Medium temperature, dissimilar patterns*, $\beta=1$, $d=0.7$: There are two equilibrium states with $r=(1-d)/2$, i.e., with $m_1=-m_2$. Each minima reproduces the distinct bits of each pattern. (d) *High temperature*, $\beta=0.5$, $d=0.7$: The only minimum is the disordered state with $r=(1-d)/2$, $p=d/2$, i.e., with $m_1=m_2=0$. All figures in this paper are presented in dimensionless units.

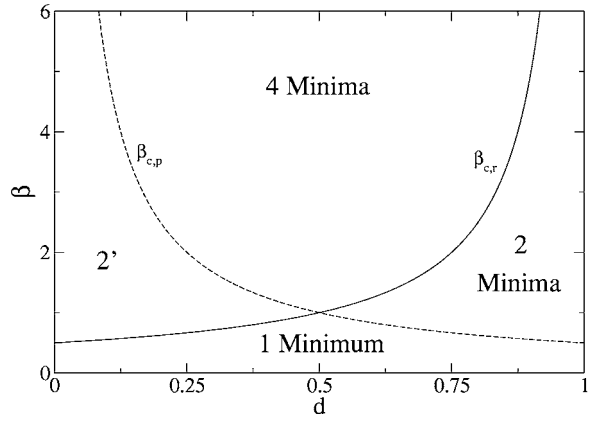


FIG. 3. Phase diagram of the system. For high $\beta$ (low temperature), the free energy has four minima. As the value of $\beta$ decreases, there are two phase transitions: one for $r$ that occurs in the first place for $d>0.5$; the other one for $p$ that takes place first for $d<0.5$. For values of $\beta$ low enough, after both transitions have occurred, the free energy is a paraboloid with only one minimum.

tive image of the first. Consequently, the system has mixed up the two patterns and it is unable to distinguish between them. The free energy landscape corresponding to this situation is plotted in Fig. 2(b).

On the other hand, if $d>0.5$, the two patterns are different enough to be distinguished even for intermediate temperatures. In this case $\beta_{c,r}>\beta_{c,p}$, and the first transition occurs at $\beta_{c,r}$. Therefore, if $\beta\in[\beta_{c,p},\beta_{c,r}]$, we have two minima with $r=(1-d)/2$, i.e., with $m_1=-m_2$. One of the two minima reproduces the distinct bits of pattern 1 and the other one the distinct bits of pattern 2. For both minima, the common bits are disordered. Although the system does not exactly reproduce the stored patterns, it perfectly distinguishes between them. The free energy in this case is plotted in Fig. 2(c).

Finally, above the maximum critical temperature, the only equilibrium state is completely disordered: $r=(1-d)/2$ and $p=d/2$, or $m_1=m_2=0$, as shown in Fig. 2(d).

The full phase diagram (Fig. 3) shows the four different phases the system can display. We will focus on the region labeled "2 minima" where each minima corresponds to one of the patterns, as opposed to region "2′", where the attractors do *not* reproduce the patterns accurately. It is also rel-

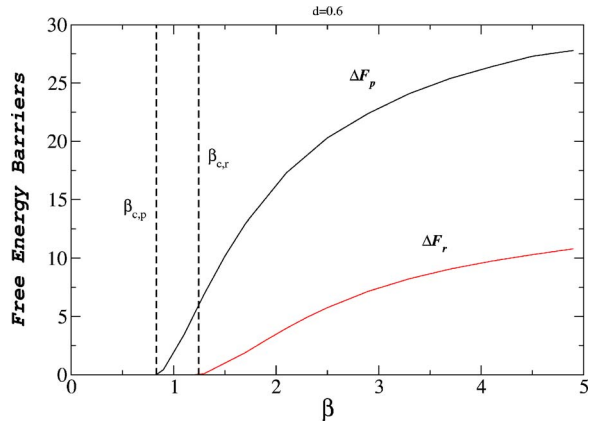


FIG. 4. (Color online) Free energy barriers $\Delta\mathcal{F}_r$ and $\Delta\mathcal{F}_p$ between the minima and the maxima, for $d=0.6$, $N=100$. As $\beta$ decreases (temperature increases), both barriers decrease continuously to zero. For this value of $d$, the first transition to take place is for the variable $r$.

evant to look at the behavior of the free energy barriers the system has to jump over to complete a transition between the minima (see Fig. 4). As $\beta$ increases (or, conversely, the temperature decreases), the barrier between the attractors is higher, making the resonance more difficult (see later). Only for values of $\beta$ between $\beta_{c,p}$ and $\beta_{c,r}$ is the system inside that region.

## IV. ANALYTICAL DERIVATION OF THE SYSTEM SIZE AMPLIFICATION

We have calculated an analytical expression for the signal amplification. Our scheme follows the general outline of the two-state model from [25,26]. The first step is to consider the time evolution of the order parameters as a stochastic process and to write a master equation for the time evolution of the order parameters, with the two-state approximation: at any time, either $m_i=m_+$ (with probability $n_+$), or $m_i=m_-$ (with probability $n_-$). The master equation is

$$\dot{n}_+ = -W_- n_+ + W_+ n_-,$$

$$\dot{n}_- = -W_+ n_- + W_- n_+, \tag{9}$$

$W_\pm(t)$ being the transition probability densities *to* the states $m_\pm$. Using the normalization condition $n_+ + n_- = 1$, Eqs. (9) can be reduced to two separated first order, linear ordinary differential equations. The problem is then solved by providing an ansatz for the transition probability densities:

$$W_\pm(t) = C\exp(-\beta\Delta\mathcal{F}) \times \begin{cases} \exp(\pm\beta N dh) & \text{if } \mu(t)=1, \\ \exp(\mp\beta N dh) & \text{if } \mu(t)=2. \end{cases} \tag{10}$$

The first exponential factor gives the purely noise-induced transition probability and the second one gives the (time-dependent) contribution of the stimulus. The factor $C$, possibly depending on $\beta$ and $d$, is the only fit parameter in the theory.

It will be useful in the following discussion to define the function:

$$W = W_+ + W_- = c\exp(-\beta\Delta\mathcal{F})\cosh(\beta h d N). \tag{11}$$

By using Fourier series, the square-wave-like form of $W_\pm$ is tackled and Eqs. (9) can be solved. The asymptotic ($t_0 \to -\infty$) solution found is

$$n_+^{as}(t) = \frac{1}{2} + \sum_{k=1}^{\infty} \frac{4C\exp(-\beta\Delta\mathcal{F})\sinh(\beta N dh)}{(2k-1)\pi\sqrt{W^2+(2k-1)^2\Omega^2}} \sin[(2k-1)\Omega t - \phi_k] \tag{12}$$

and the total exact solution is

$$n_+(t) = n_+^{as}(t) + \exp[-W(t-t_0)] \times \left\{ \delta_{m_0,m_+} - \sum_{k=1}^{\infty} \frac{4C\exp(-\beta\Delta\mathcal{F})\sinh(\beta N dh)}{(2k-1)\pi\sqrt{W^2+(2k-1)^2\Omega^2}} \sin[(2k-1)\Omega t_0 - \phi_k] - \frac{1}{2} \right\}. \tag{13}$$

From Eq. (13) it is possible to obtain the time-dependent moments of the order parameters, and particularly the first two moments $\langle m(t)\rangle$ and $\langle m(t)m(t+\tau)\rangle$. The second moment, or self-correlation, is particularly important since, by using Wiener-Khinchin theorem [27], we can obtain the power spectra $S_m(\omega)$ and the signal amplification $\eta$. However, the physically meaningful result is the time average of the self-correlation:

$$\overline{\langle m(t)m(t+\tau)\rangle} = \frac{\Delta^2}{4}\left\{1-\tanh^2(\beta N dh) \times \left[1-\frac{2\Omega}{\pi W}\tanh\left(\frac{\pi W}{2\Omega}\right)\right]\right\} \times \exp(-W\tau) + \frac{\Delta^2}{2\pi^2}\tanh^2(\beta N dh) \times \sum_{k=1}^{\infty} \frac{W^2\cos[(2k-1)\Omega\tau]}{(2k-1)^2[W^2+(2k-1)^2\Omega^2]} + \frac{(m_+ + m_-)^2}{4}, \tag{14}$$

where the overline denotes time averaging.

The final expression for the power spectrum, from the Wiener-Khinchin theorem, is

$$\mathcal{S}_m(\omega) = \frac{\Delta^2}{4}\left\{1-\tanh^2(\beta h d N) \times \left[1-\frac{2\Omega}{\pi W}\tanh\left(\frac{\pi W}{2\Omega}\right)\right]\right\}\frac{2W}{\omega^2+W^2} + \frac{2\Delta^2}{\pi}\tanh^2(\beta h d N)\sum_{k=1}^{\infty}\frac{W^2}{(2k-1)^2[W^2+(2k-1)^2\Omega^2]}$$

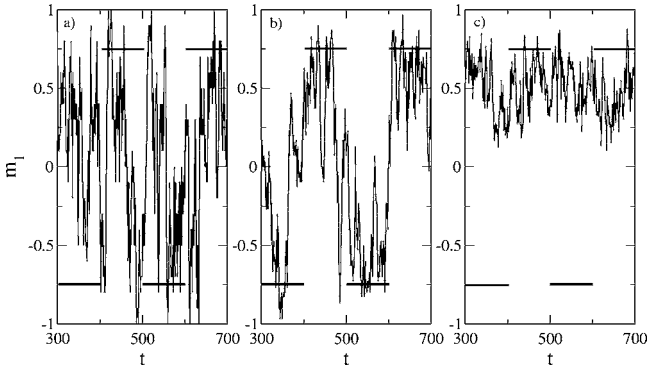


FIG. 5. The graph shows the time evolution of the order parameter $m_1$. The first evidence of system-size resonance is clear. The solid thin line is the order parameter obtained from numerical simulations. The thick segments show the time intervals in which the external stimulus drives the system to retrieve one or the other pattern. The parameters values are $\beta=1.2$, $d=0.6$, $T=100$, and $h=0.01$. (a) $N=20$; (b) $N=60$; and (c) $N=120$.

$$\times (\delta[\omega-(2k-1)\Omega]+\delta[\omega+(2k+1)\Omega]) + \frac{\pi(m_+ + m_-)^2}{2}\delta(\omega). \tag{15}$$

The free-energy barrier between the attractors, $\Delta\mathcal{F}$, needs to be calculated in order to solve the problem. The extrema of Eq. (7) are obtained by minimizing $\mathcal{F}$ numerically for every value of $N$, $d$, and $\beta$. The analytical curves in Figs. 6 and 10 are obtained fitting these numerical values to an expression linear in $N$. One can observe a good agreement between the numerical and analytical results. We also obtained from this minimization process the distance between the attractors, denoted by $\Delta$.

$$\eta = \lim_{\Delta\omega\to 0} \frac{2\int_{\Omega-\Delta\omega}^{\Omega+\Delta\omega} S_m(\omega)d\omega}{h^2} = \frac{2\Delta^2}{\pi h^2}\tanh^2(\beta h d N)\frac{W^2}{(W^2+\Omega^2)}. \tag{16}$$

The quantity, $\eta$, in Eq. (16) presents our measure of stochastic resonance [3,5].

## V. RESULTS

To complete the analysis, we have also performed out-of-equilibrium Monte Carlo simulations [24] of the Hamiltonian (1). We have used the standard Metropolis acceptance rates in a single spin-flip update scheme. We have simulated 100 000 sweeps of the time evolution of the system for every parameter set. In order to compare with the theoretical results, the order parameters $m_i(t)$ as functions of time are obtained from the simulation. The power spectra, $S_m(\omega)$, and the signal amplification $\eta$ [3] are then evaluated.

In a certain range of parameter space, the numerical simulations performed show the presence of SSR effects in the model (1). A relevant example is presented in Fig. 5. The intuitive explanation of the performance of the system is the following. For small $N$, the fluctuations are strong, therefore the system output is too noisy and the system is unable to retrieve the patterns in real time. The hopping between the attractors is random and not synchronized with the shifts in the external stimulus. For very large $N$, the fluctuations are weak and the system resides in a given attractor for too long, while the stimulus has performed several shifts. However, for intermediate values of $N$ around the optimal value, the system follows the oscillations of the external stimulus and the appropriate pattern for every half-period is retrieved very precisely.

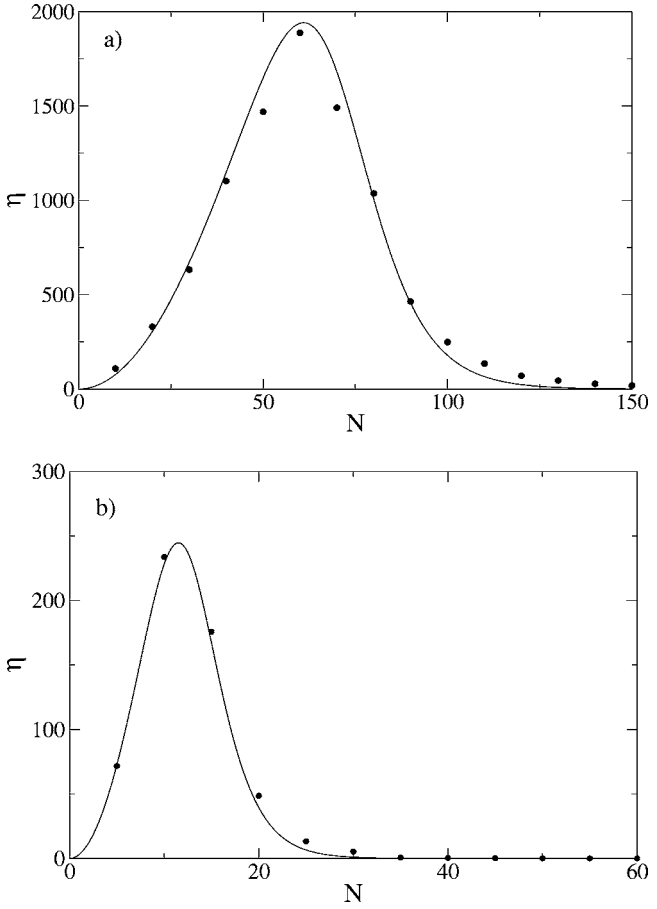


FIG. 6. The signal amplification, $\eta$, vs the size of the system, $N$. The result of the numerical simulation is represented by dots while the analytical result is the solid line. $T=500$, $\beta=1.2$, and $h=0.01$. (a) $d=0.6$ and (b) $d=0.8$. For larger values of $d$, the maximum is shifted to the left.

The resonant behavior of the signal amplification is presented in Fig. 6. It is clear from the figure that there is a maximum of the signal amplification at a finite intermediate size. The results of the numerical simulation (dots) match very precisely the analytical curve (solid line), given by Eq. (16).

The difference between both panels of Fig. 6 is due to a different value of $d$, while the other parameters $\Omega$, $h$, and $\beta$ are equal. A larger value of $d$ implies a higher energy barrier between the attractors, see Eq. (7). Therefore a larger noise intensity is needed to achieve the maximum of the resonance. This larger noise requires smaller values of $N$. There-

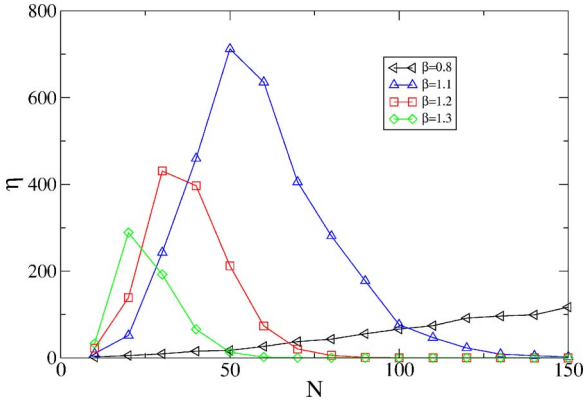


FIG. 7. (Color online) The effect of the temperature on $\eta$. In this plot, $d=0.6$, $T=100$, and $h=0.01$. For values of $\beta$ smaller than $\beta_{c,p}=0.833$, there can be no resonance, $\beta=0.8$, left triangles. Below the critical point, the higher the temperature, the stronger the resonance is. $\beta=1.1$, up triangles; $\beta=1.2$, squares; even in the region of four minima, for values of $\beta$ higher than $\beta_{c,p}=1.25$ ($\beta=1.3$, up-triangles) the resonance is present. Higher values of $\beta$ would maximize the resonance for smaller values of $N$ until the resonance disappears for high enough $\beta$.

fore the maximum of $\eta$ is shifted towards smaller $N$, and its maximum value, achieved in the resonance, is reduced.

It is also interesting to study the response of the system as a function of the other relevant parameters $\beta$, $d$, and $\Omega$. We now proceed to comment on the different results obtained concerning these dependencies. It is to be expected that increasing the temperature (decreasing $\beta$) will enhance the effect, shifting the maximum towards higher $N$, in order to keep the effective noise intensity $(\beta N)^{-1}$ constant. However, this tendency has its limits: we must operate below the critical point to observe bistable behavior and, therefore, SSR (see Fig. 7). On the other hand, decreasing the temperature (increasing $\beta$) will force the maximum towards lower $N$ and, eventually, the resonance disappears.

The effect of changing $d$ is even more interesting. In Fig. 8 it is visible that there is also resonant behavior as a function of $d$. In the graph, $\eta$ is normalized by $d^2$ to take into account that, given that the distance between attractors $\Delta$ is approximately $2d$, the amplitude in the oscillations of the order parameters is also of order $2d$. Therefore $\eta$ is proportional to $d^2$ as a null hypothesis. Even when this trivial dependency is removed, an optimal $d$ is observed for every value of $N$ and $\beta$ and the functional form of the dependency tends to a certain curve in the thermodynamic limit. This resonant behavior appears due to the modulation in the energy landscape introduced by $d$. Since the energy barrier between the attractors can be demonstrated to depend quadratically on $d$, changing $d$ modulates the factor $\beta\Delta\mathcal{F}$ as if we were changing the noise intensity relative to $\Delta\mathcal{F}$. Therefore it is to be expected to observe an increased response as well as a shifting of the maxima to the left, when $N$ is increased.

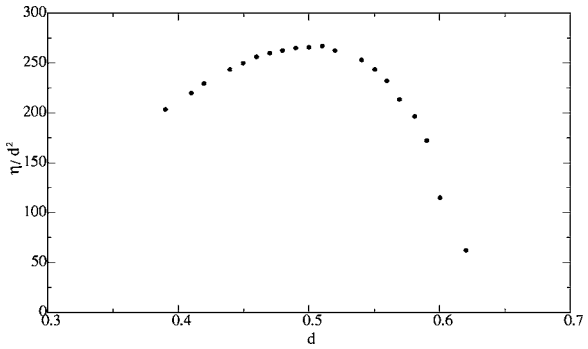


FIG. 8. The resonant behavior of $\eta$ as a function of $d$ (see text for more details). $T=100$, $N=100$, $\beta=1.2$, and $h=0.1$.

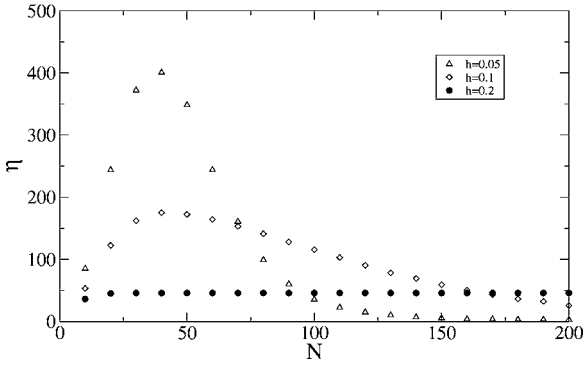


FIG. 9. Spectral amplification vs $N$ for different values of the stimulus intensity, $h$. As $h$ increases from low values, the resonant peak becomes wider and lower until the resonance disappears. $T=100$, $\beta=1.2$, and $d=0.6$.

The resonant behavior is strongest, as usual when dealing with stochastic resonance, for small values of the external stimulus, $h$ (see Fig. 9). Higher values of $h$ diminish the effect until it entirely disappears for high enough $h$.

Finally the dependence of $\eta$ on the stimulus frequency $\Omega$ is shown in Fig. 10. It shows the Lorentzian dependence expected in SR [25,28]. The good agreement between theory and numerical simulations is observed as well.

## VI. CONCLUSIONS

In this paper we presented theoretical calculations, based on a two-state model, showing the presence of system size resonance (SSR) effects in attractor neural networks. The

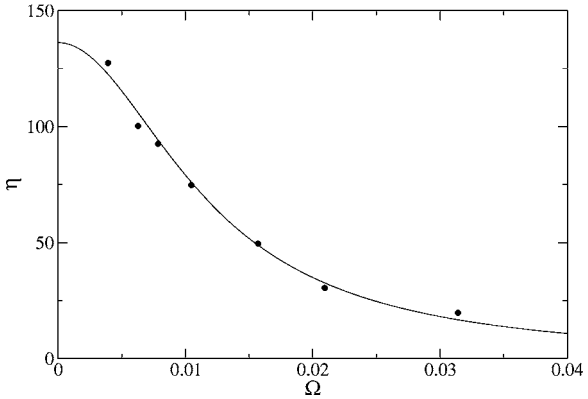


FIG. 10. The behavior of $\eta$ with the frequency of the external stimulus, $\Omega$ shows the expected Lorentzian form, as in usual stochastic resonance. Again, the dots represent the numerical simulations and the solid line the analytical results. In this plot, $d=0.6$, $N=50$, and $\beta=1.2$.

only approximation required is the two-state assumption, all other information is obtained from exact thermodynamical calculations. The results have been also compared with Monte Carlo simulations and we have found a very good agreement. The resonance is made evident by the behavior of the signal amplification $\eta$ as a function of the size of the system as well as by the time evolution of the order parameters. Therefore, for a given external, time-dependent stimulus, there is an optimal size of the network in which there is maximal synchronization of the system to the evolving stimulus.

The behavior of $\eta$ versus the other relevant parameters of the system was also studied. As expected from the results of [5], the resonance only appears in the ferromagnetic phase, for high enough inverse temperature $\beta$. The dependence with the frequency of the external stimulus $\Omega$ is the expected Lorentzian one. Also in accordance with the previous literature [25], the resonance is only present for the small amplitude of the stimulus $h$. A unique feature of SSR in attractor neural networks is the peculiar nonmonotonous behavior of $\eta$ versus the Hamming distance $d$, which is, however, another natural consequence of the presence of SSR in the system.

## ACKNOWLEDGMENTS

This work was financially supported by Ministerio de Ciencia y Tecnología (Spain), Projects No. BFM2001-291 and No. FIS2004-271, and by UNED, Plan de Promoción de la Investigación 2002.

[1] W. Horsthemke and R. Lefever, *Noise-Induced Transitions* (Springer-Verlag, Berlin, 1984).
[2] J. García-Ojalvo and J. M. Sancho, *Noise in Spatially Extended Systems* (Springer-Verlag, New York, 1999).
[3] P. Jung and P. Hänggi, Phys. Rev. A **44**, 8032 (1991).
[4] R. Benzi, A. Sutera, and A. Vulpiani, J. Phys. A **14**, 453 (1981).
[5] A. Pikovsky, A. Zaikin, and M. A. de la Casa, Phys. Rev. Lett. **88**, 050601 (2002).
[6] R. Toral, C. R. Mirasso, and J. D. Gunton, Europhys. Lett. **61**, 162 (2003).
[7] G. Schmid, I. Goychuk, P. Hänggi, S. Zeng, and P. Jung, Fluct. Noise Lett. **4**, L33 (2004).
[8] M. S. Wang, Z. H. Hou, and H. W. Xin, Chem. Phys. Chem. **5**, 1602 (2004).
[9] Z. H. Hou and H. W. Xin, Chem. Phys. Chem. **5**, 407 (2004).
[10] H. Hong, B. J. Kim, and M. Y. Choi, Phys. Rev. E **67**, 046101 (2003).
[11] Y. Z. Shao, W. R. Zhong, G. M. Lin, and J. C. Li, Acta Phys. Sin. **53**, 3157 (2004).
[12] H. S. Wio, e-print cond-mat/0410464.
[13] C. J. Tessone and R. Toral, e-print cond-mat/0409620.
[14] L. M. Ward, Fluct. Noise Lett. **4**, L11 (2004).
[15] J. K. Douglass, L. Wilkens, E. Pantazelou, and F. Moss, Nature (London) **365**, 337 (1993).
[16] E. Simonotto, M. Riani, C. Seife, M. Roberts, J. Twitty, and F. Moss, Phys. Rev. Lett. **78**, 1186 (1997).
[17] D. F. Russell, L. A. Wilkens, and F. Moss, Nature (London) **402**, 291 (1999).
[18] I. Hidaka, D. Nozaki, and Y. Yamamoto, Phys. Rev. Lett. **85**, 3740 (2000).
[19] J. Hopfield, Proc. Natl. Acad. Sci. U.S.A. **79**, 2554 (1982).
[20] D. Hebb, *The Organization of Behavior: A Neurophysiological Theory* (Wiley, New York, 1949).
[21] M. Mezard, G. Parisi, and M. Virasoro, *Spin-Glass Theory and Beyond* (World Scientific, Singapore, 1987).
[22] V. Privman, *Finite-Size Scaling and Numerical Simulations of Statistical Systems* (World Scientific, Singapore, 1990).
[23] D. J. Amit, H. Gutfreund, and H. Sompolinsky, Phys. Rev. A **32**, 1007 (1985).
[24] M. E. J. Newman and G. T. Barkema, *Monte Carlo Methods in Statistical Physics* (Clarendon Press, Oxford, 1999).
[25] L. Gammaitoni, P. Hänggi, P. Jung, and F. Marchesoni, Rev. Mod. Phys. **70**, 223 (1998).
[26] B. McNamara and K. Wiesenfeld, Phys. Rev. A **39**, 4854 (1989).
[27] C. W. Gardiner, *Handbook of Stochastic Methods* (Springer-Verlag, Berlin, 1983).
[28] P. Jung, Phys. Rep. **234**, 175 (1993).